Wave transport in stealth hyperuniform materials: The diffusive regime and beyond

Élie Chéron, Simon Félix, Jean-Philippe Groby, Vincent Pagneux, Vicente Romero-García

Wave transport in stealth hyperuniform materials: the diffusive regime and beyond

Élie Chéron,[1] Simon Félix,[1] Jean-Philippe Groby,[1] Vincent Pagneux,[1] and Vicente Romero-García[1, a)]

Laboratoire d'Acoustique de l'Université du Mans (LAUM), UMR 6613,

Institut d'Acoustique - Graduate School (IA-GS), CNRS, Le Mans Université, Le Mans,

France

(*Electronic mail: Jean-Philippe.Groby@univ-lemans.fr)

(Dated: 11 July 2022)

By varying the degree of correlation in stealthy hyperuniform (SHU) materials, the continuous evolution from uncorrelated disorder to periodic media is possible and allows, as such, to study the fate of the bimodal distribution, characteristic of a diffusive transport. Considering the wave transport through a SHU distribution of a given number of scatterers and at a given frequency, the transition from a diffusive to a transparent medium is clearly observed only below the Bragg frequency. This transition is characterized by a threshold value of the stealthiness, at the vicinity of which the material abruptly changes from diffusive to transparent. Contrastingly, no such clear transition is observed at or above the Bragg frequency and, surprisingly, a seemingly-bimodal distribution of the transmission eigenvalues still characterizes the SHU materials, even when strongly correlated.

[a)]Also at Instituto Universitario de Matemática Pura y Aplicada, Departamento de Matemática Aplicada, Universitat Politècnica de València, Camino de Vera s/n, 46022, València, Spain

Wave transport in stealth hyperuniform materials: the diffusive regime and beyond

Interferences play an essential role in wave transport through complex heterogeneous media. They give rise to phenomena that prevail in the scattering properties of such media and open up numerous applications for wave control. Enhanced backscattering, conductance fluctuations, or the Anderson localization in disordered media[1–3], as well as the band structure of the transmission spectrum in periodic media[4,5], are well-known examples of interference induced phenomena. Another striking example is the bimodal distribution of the transmission eigenvalues (TEV) in the transport through a diffusive disordered medium[6–14]. The TEV distribution $P(\tau)$ indeed exhibits two peaks corresponding to closed, almost fully reflected, eigenchannels ($\tau \to 0$) and open, almost fully transmitted, eigenchannels ($\tau \to 1$). Of particular interest are the latter, which existence implies, that, given a sufficiently controlled pattern of the incident wave, it can be transmitted with almost no energy loss through an otherwise opaque medium. This counter-intuitive effect has given rise to the wavefront shaping technique, following a first experimental evidence by Vellekoop and Mosk[15].

Between the limit cases of fully disordered or perfectly crystalline media, correlated materials, that is, scattering systems which disorder displays spatial correlations, have emerged as new possibilities to control waves[16–19] and design functional materials[20,21]. Also, one may wonder about the fate of the bimodal property when introducing correlations, especially since this property will no longer be observed in strongly correlated, crystalline, structures, which will rather be fully opaque or transparent due to Bragg scattering.

A good candidate to investigate the continuous transition from diffusive to transparent materials is the class of hyperuniform materials[22]. Hyperuniform materials are made of a discrete distribution of scatterers on a correlated point pattern, the long-range density fluctuations of which vanish. In Fourier space, this translates in a vanishing structure factor $S(\mathbf{q})$ when $|\mathbf{q}| \to 0$. A particular class of hyperuniform materials, which we will consider in this paper, is that of stealthy hyperuniform (SHU) materials, for which the structure factor vanishes on a finite domain $|\mathbf{q}| < q_\mathrm{c}$, the bound of which depends on a stealthiness parameter, χ (see below), that allows us to continuously tune the material from fully disordered to perfectly ordered[23–35]. As a consequence, the material is transparent to long-wavelength incident waves under the assumption of single scattering. Experimental evidences of this kind of structures has been recently shown for airborne acoustic[36,37] as well as for electromagnetic waves[17,32,38].

In this work, we investigate the transition from uncorrelated disorder to periodic media by

Wave transport in stealth hyperuniform materials: the diffusive regime and beyond
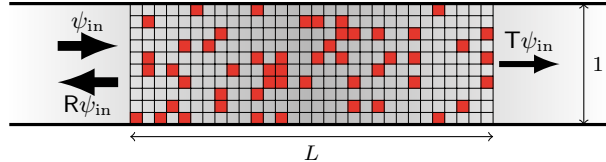

FIG. 1. Schematic representation of the scattering of a wave impinging on a random distribution of scatterers in a quasi-one-dimensional waveguide. For the sake of simplicity and computational efficiency, the scatterers (red squares) are located on a regular grid, and a full wave numerical solution[37] gives the scattering matrix of the L-length disordered slab.

considering the transmission of waves in a quasi-one-dimensional disordered waveguide. On a L-length segment of an otherwise homogeneous waveguide with unit width (Fig. 1), local heterogeneities are created by changing the material parameters on a set of randomly chosen sites of a regular grid (red squares).

Namely, the wave equation reads

$$\text{div}(a(\mathbf{r})\nabla\psi) + k^2 b(\mathbf{r})\psi = 0, \tag{1}$$

with $a = b = 1$ in the background medium of wavenumber k and $a \ll 1$, $b \ll 1$ in the scatterers. Small values of a and b are chosen so that the scatterers behave as acoustically rigid obstacles (or as perfectly conducting obstacles if ψ is a TM-polarized magnetic field travelling in the waveguide), hence without resonant behaviour. With the waveguide supporting N propagating modes, the $N \times N$ transmission matrix T of the disordered slab is computed and used to characterize the wave transport (see[37] for details on the numerical computation).

The scatterers are located on the grid as follows: (i) a 2D SHU distribution of N_s points on a $L_s \times L_s$ square area is first generated following the procedure proposed by Froufe-Pérez et al.[28] (see below), (ii) this distribution is then scaled to a $L \times L$ area, so as to keep constant the characteristic length $d = L/\sqrt{N_s}$, that is, the typical distance between the points, (iii) a subset of the point distribution that belongs to a $L \times 1$ rectangular area is extracted, (iv) the distribution of the nearest square sites on the grid is associated to the point distribution. Note that the mesh size is taken small enough (typically, 10^{-2}) to ensure that this shifting of the points on the regular grid has no significant effect on the SHU pattern properties.

The algorithm proposed in[28] starts from a random distribution of points $\{\mathbf{r}_j\}$, $j \in [1, N_s]$, in a square box and uses a simulated annealing relaxation scheme to find a pattern with a minimized
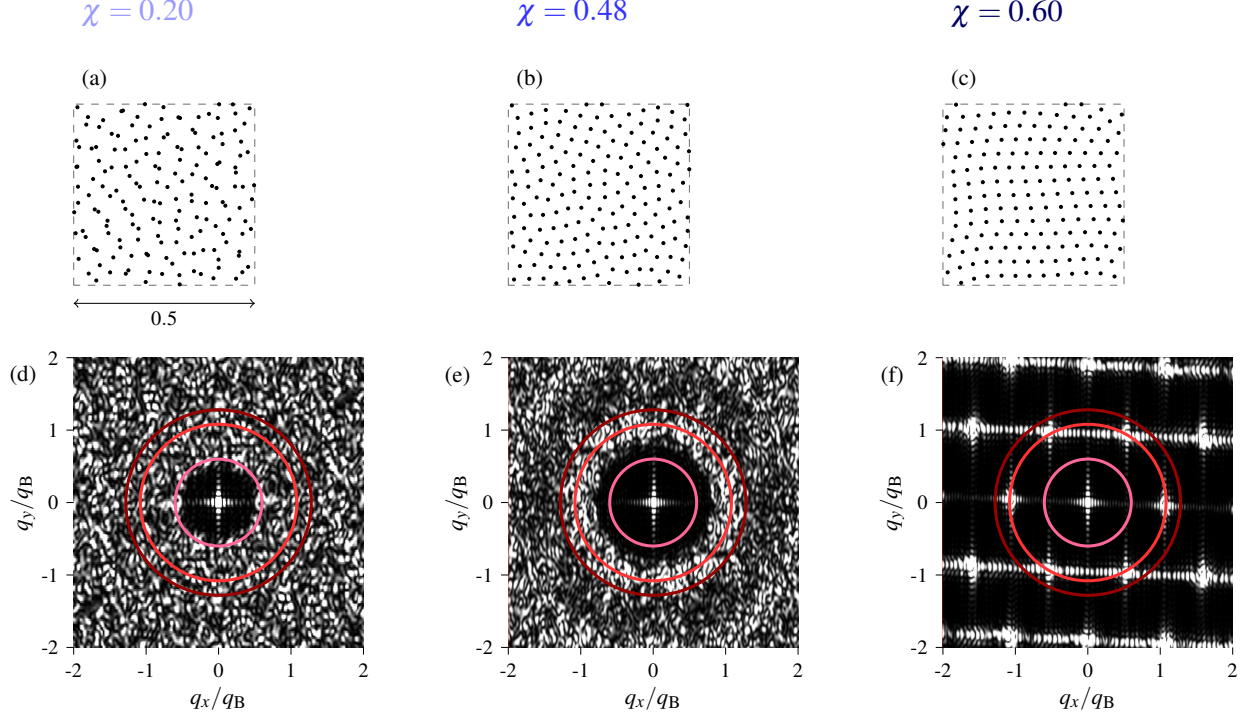
Wave transport in stealth hyperuniform materials: the diffusive regime and beyond

FIG. 2. (a,b,c) typical configurations of two-dimensional SHU point patterns for increasing values of the stealthiness ($\chi = 0.2$, 0.48, and 0.6), obtained as detailed in Ref.[28]. (d,e,f) corresponding structure factor $S(\mathbf{q})$, as estimated by the spatial Fourier transform of a pattern having the dimensions $(L, 1)$ of the slab in Fig. 1, with $L = 3$ (it is thus made of approximately 2000 scatterers). On each plot, the pink, red and dark red circumferences represent the chosen observation frequencies, $k/k_B = 0.6$, 1.08, and 1.28, see Fig. 3.

structure factor in the reciprocal domain $|\mathbf{q}| < q_c$:

$$S(\mathbf{q}) = \frac{1}{N_s} \left| \sum_{j=1}^{N_s} e^{i\mathbf{q}\cdot\mathbf{r}_j} \right|^2 < \varepsilon, \tag{2}$$

with, typically, $\varepsilon = 10^{-6}$. The degree of positional correlation of the generated pattern can be encoded by the stealthiness χ:

$$\chi = \frac{M(q_c)}{2(N_s - 1)}, \quad M(q_c) = \frac{1}{2}\frac{\pi q_c^2}{(2\pi/L_s)^2}, \tag{3}$$

which is the ratio of the number of constrained degrees of freedom, $M(q_c)$, over the total number of degrees of freedom, $2(N_s - 1)$ (upon removing the translational degrees of freedom). The lower bound $\chi = 0$ corresponds to an uncorrelated disordered distribution. Figures 2(a-c) show typical patterns of SHU points distributions at low ($\chi = 0.20$), mid ($\chi = 0.48$), and higher ($\chi = 0.60$) values of the stealthiness, revealing a gradually increasing order. The SHU system crystallizes
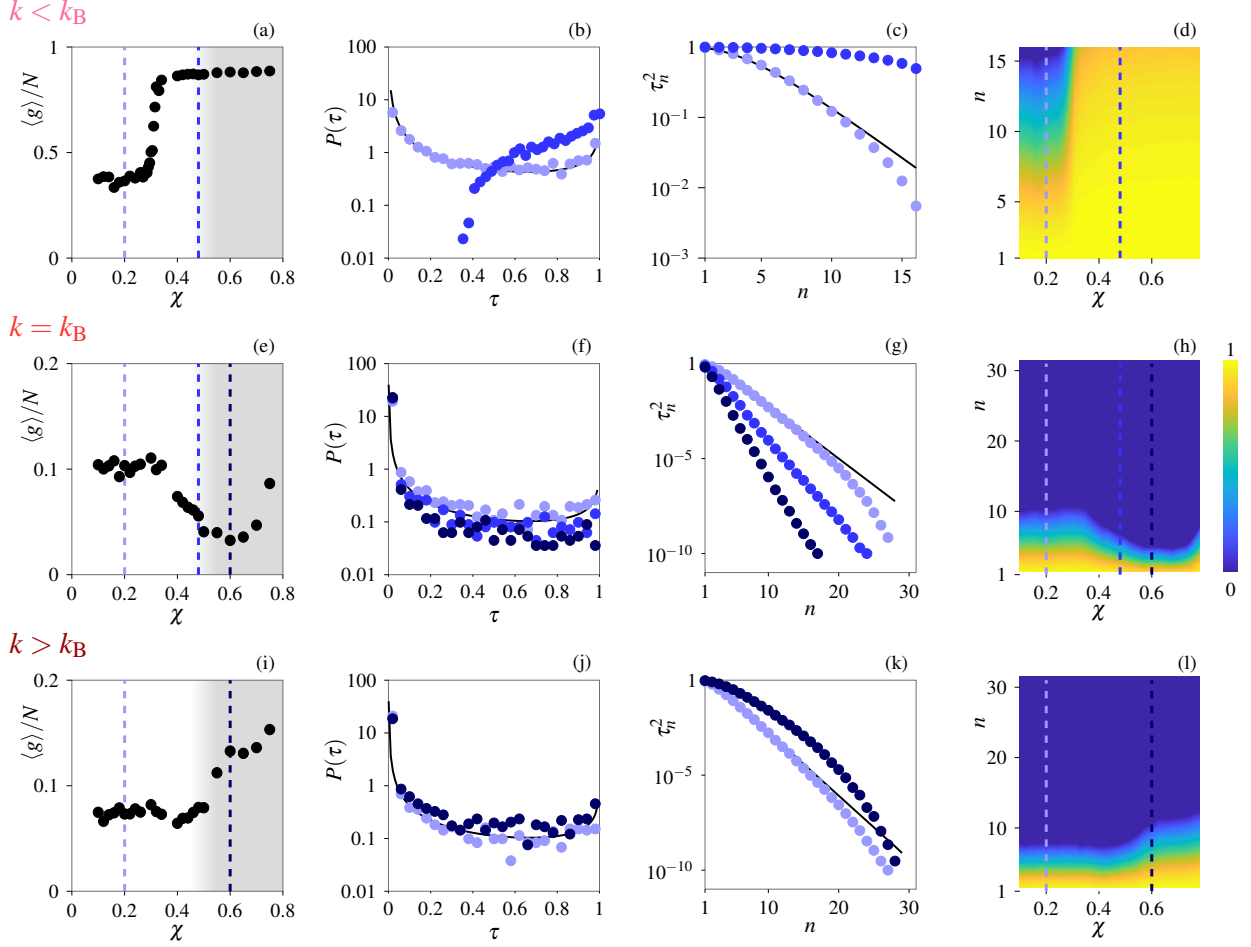
FIG. 3. Transmission through a slab of scatterers with correlated disorder, at a frequency below the Bragg frequency k_B (first row, a-d), at k_B (second row, e-h), and above k_B (third row, i-l). First (left) column: conductance, averaged over 100 realizations, as a function of the stealthiness χ. Second column: TEV distribution $P(\tau)$ (normalized) for selected values of χ, shown as dashed blue lines in the first column plots. The black solid line shows the theoretical bimodal distribution 5. Third column: TEV τ_n^2 for the same values of χ, ordered by decreasing values, with comparison to the bimodal relation 6. Fourth column: TEV τ_n^2, as a function of the stealthiness χ and index n.

into a square lattice when $q_c = q_B = 2\pi/d$, corresponding to a maximum value of the stealthiness $\chi_{max} \simeq \pi/4$ for large N_s (sets of approximately 6000 points were generated for the following numerical results).

Figures 2(d-f) show the corresponding structure factor $S(\mathbf{q})$ as estimated by the spatial Fourier transform of the $L \times 1$ distribution of scatterers aligned to the grid, with $L = 3$ (it is thus made of approximately 2000 scatterers). For a low degree of correlation ($\chi = 0.20$), the constrained region
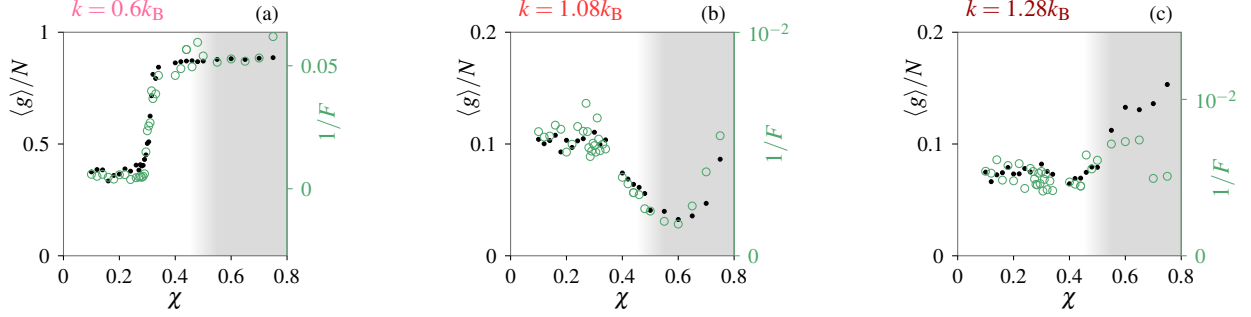
5

FIG. 4. Averaged conductance, as shown in Fig. 3(a,e,i), compared with the inverse of the integrated structure factor $F(q = \alpha q_B, \chi)$, with (a) $\alpha = 0.6$, (b) $\alpha = 1.08$, (c) $\alpha = 1.27, 1.28, 1.29$.

$|\mathbf{q}| < q_c$ clearly appears and the surrounding region displays a global isotropy. SHU structures remain isotropic up to $\chi \simeq 0.5$, while $S(\mathbf{q})$ locally increases around $|\mathbf{q}| = q_B$, as a precursor signature of the Bragg scattering characteristic of periodic media, see Fig. 2(e). A second local increase near $|\mathbf{q}| = 2q_B$ is observed. Above $\chi = 0.5$, the structures are no longer isotropic, see Fig. 2(f), and a discrete pattern, characteristic of a crystalline structure, gradually appears.

Let us place the generated disordered distributions of scatterers in a waveguide, as shown in Fig. 1, and analyze how the disorder correlation affects the transmission, depending on the frequency of the incident wave. To do this, three frequencies are chosen as depicted on Figs. 2(d-f) by the pink, red, and dark red circumferences. Note that these circumferences depict the frequencies in a reduced form k/k_B, with $k_B = q_B/2 = \pi/d$, as a consequence of the von Laue condition for scattering[39] (see, e.g.,[40] for details). For χ small enough, the three chosen frequencies "lie" in the unconstrained region, see Fig. 2(d) and thus a classical diffusive transport is expected. For larger values of χ, the transport in a strongly correlated medium, and consequently the transition from disorder to order, is more sensitive to the frequency, and in particular to its relative value to the Bragg frequency k_B.

The first frequency, $k = 0.6k_B$ (pink circumfrence), is chosen below the Bragg frequency, such that, for χ large enough (namely, above $\chi = 0.6^2\chi_{max} \simeq 0.3$), this frequency lies in the constrained region and the medium is then expected to be transparent. This is indeed what is observed when plotting the Landauer conductance $g = \text{Tr}(\mathsf{T}\mathsf{T}^\dagger)$ from Ref. [41] as a function of the stealthiness, see Fig. 3(a), where T represents the transmission matrix of the system.

The conductance is first relatively small ($\langle g \rangle/N \simeq 0.3$, here averaged over 100 realizations of the scatterer distribution), as typically observed in the diffusive transport, and reaches a high

Wave transport in stealth hyperuniform materials: the diffusive regime and beyond

plateau for larger values of χ. Note that the conductance does not reach its maximum value, $\langle g \rangle / N = 1$, although transparency is expected. This is due to the alignment of the point pattern on the regular grid (see above), the consequence of which is a structure factor that is not perfectly zero in the constrained region, hence a non perfect transmission. Between these two limits (diffusive and transparent), the transition is abrupt. Note that a scale of this transition width with χ can be deduced from the initial point pattern. Indeed, consider an integrated structure factor

$$F(q,\chi) = \sum_{|\mathbf{q}|=q} S(\mathbf{q},\chi), \tag{4}$$

the inverse of which is expected to be low in regions of strong scattering and large in the regions of weak scattering, as is the transmission. Figure 4(a) shows that $F^{-1}(q,\chi)$ displays the same abrupt transition for $k < k_{\mathrm{B}}$ (analogously, $q < q_{\mathrm{B}}$) and compares well with the conductance.

For a weakly correlated disorder, a characteristic property of the diffusive transport is that the TEV follow the bimodal distribution

$$P(\tau) = \frac{N\ell}{L+\ell} \frac{1}{\tau\sqrt{1-\tau}}, \tag{5}$$

with ℓ the transport mean free path, as shown in Fig. 3(b), or, equivalently, in Fig. 3(c), with the TEV following

$$\tau_n = \frac{1}{\cosh^2{(n/\bar{n})}}, \tag{6}$$

with $\bar{n}$ adjusted to meet $\sum_{n=1}^{N} \cosh^{-2}(n/\bar{n}) = \langle g \rangle$[6,11,42]. Above the threshold value $\chi \simeq 0.3$ - an example is given in Figs. 3(b-c) for $\chi = 0.4$ - the TEV distribution no longer follows the bimodal distribution and no closed eigenchannel is observed, resulting in the strongly increased transparency of the medium. Figure 3(d) shows the distributions of TEV, τ_n, as functions of the index n and stealthiness χ: the abrupt transition from the diffusive to the transparent regime clearly appears.

Close to the Bragg frequency k_{B} (red circumference in Fig. 2), the effect of increasing the disorder correlation on the transmission significantly differs from that observed at lower frequencies. Figure 3(e) shows the evolution of the averaged conductance with the stealthiness. While the medium still behaves as a diffusive medium for low values of χ, with the conductance following the Ohm's law $\langle g \rangle / N = \ell / (L+\ell)$[43], the Bragg scattering, consequence of the progressive crystallization of the medium, makes the averaged transmission decrease near $\chi \simeq 0.5$. Above $\chi \simeq 0.6$, the anisotropy of the hyperuniform medium makes the transmission strongly dependent on the incident field direction, or, in our case, on the realization of the randomly generated slab in

7

Wave transport in stealth hyperuniform materials: the diffusive regime and beyond

the waveguide: the medium can be either strongly reflecting or almost transparent. This relates to the structure factor shown in Fig. 2(f). Near $|\mathbf{q}| = q_B$ (red circumference) the structure factor may be close to zero or have larger values (Bragg peaks), depending on the orientation of the wavevector. When averaging over the angles, the integrated structure factor $F(q \simeq q_B, \chi)$ decreases with increasing χ in the crystalline regime ($\chi > 0.6$, see Fig. 4(b)). This decrease can be associated to the increase of the average conductance in Fig. 3(e). Remarkably, a bimodal distribution of the TEV is still observed when varying the stealthiness, see Figs. 3(f-h). Regardless of the disorder correlations, the eigenchannels are predominantly closed or open.

In the last case considered (dark red circumferences in Fig. 2), when the frequency is higher than the Bragg frequency, the wavevector always lies in the unconstrained region. A consequence is that the value of the conductance remains roughly that in a fully diffusive medium, until the transition from disordered to crystalline, that is, around $\chi \simeq 0.5$, see Fig. 3(i). Then, the same averaging induced effect as discussed above leads to an increase of the transmission with the stealthiness in crystallized SHU media. Note that, above $q = q_B$ and for large χ, the evolution of the structure factor no longer follows that of the conductance above $k = k_B$, see Figs. 4(c). Figure 2(f) might explain this: the Fourier transform, performed over a finite $L \times 1$ spatial domain with finite size scatterers, displays secondary maxima whereas the Fourier transform of an infinite periodic distribution of points, ideally giving the structure factor, would appear pointwise. Consequently, the integrated structure factor, taken as an indicator of the scattering by the medium,
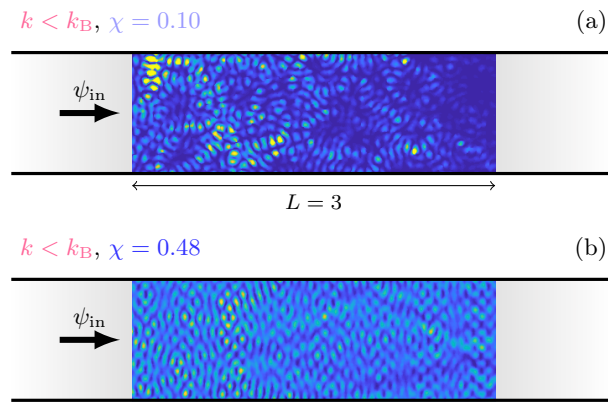

FIG. 5. (a) Amplitude of a typical wavefield in a SHU medium with low stealthiness and a a frequency below the Bragg frequency, illustrating a characteristic diffusive transport. (b) At the same frequency, amplitude of a typical wavefield in a SHU medium with a larger stealthiness such that the medium is almost transparent. The incident wave, ψ_{in}, is a plane wave.

possibly overestimates this scattering.

Note, finally, that a bimodal distribution of the TEV is still observed when $k > k_{\mathrm{B}}$, regardless of the stealthiness. Thus, although the bimodal distribution is usually known as a characteristic of the diffusive transport in a fully disordered medium, it seems that, considering SHU media, fulfilling a bimodal law is the rule, and breaking it, the exception.

Figures 5(a) and (b) show two snapshots for $k < k_{\mathrm{B}}$ of the acoustic field through two SHU distributions with $\chi = 0.10$ and $\chi = 0.48$ respectively. As discussed before in Figs. 3 and 4, the random scattering for the SHU distribution with $\chi = 0.10$ at the $k < k_{\mathrm{B}}$ makes the material almost opaque, as the conductance and, as a consequence, the transmission is very low. However, for the SHU distribution with $\chi = 0.48$ at the $k < k_{\mathrm{B}}$, the material is transparent before the transition from diffusive to transparent media.

We have analyzed the continuous transition from the diffusive transport through an uncorrelated disorder to the transparency or Bragg scattering in an ordered, periodic, medium. This transition is achieved by using stealthy hyperuniform distributions of rigid scatterers in a waveguide, with a controlled and adjustable stealthiness. A first remarkable observation is, at sufficiently low frequency - namely, below the Bragg frequency - an abrupt transition from diffusive to transparent is observed. A threshold value of the stealthiness, frequency dependent, separates media that are mostly opaque for the incident wave, as illustrated in Fig. 5(a), from media that are almost transparent, see Fig. 5(b). The mechanism and typical scale of this sharp transition, although not fully explained with the present work, can be related to the structure factor of the spatial distribution of the scatterer locations. The results shown here can be used for the material design as elements to control both the diffusivity and the transparency of the material. It is also noticeable that the bimodal distribution of the transmission eigenvalues appears as a general property of the propagation through the SHU medium and not solely as a characteristic of the diffusive transport.

ACKNOWLEDGMENTS

Wave transport in stealth hyperuniform materials: the diffusive regime and beyond

DATA AVAILABILITY STATEMENT

The data that support the findings of this study are available from the corresponding author upon reasonable request.

REFERENCES

[1] E. Akkermans and G. Montambaux, *Mesoscopic physics of electrons and photons* (Cambridge University Press, 2007).

[2] A. García-Marín and J. J. Sáenz, "Statistical properties of wave transport through surface-disordered waveguides," Wave Random Complex **15**, 229 (2005).

[3] S. Rotter and S. Gigan, "Light fields in complex media: Mesoscopic scattering meets wave control," Rev. Mod. Phys. **89**, 015005 (2017).

[4] J. D. Joannnopoulos, S. G. Johnson, J. N. Winn, and R. D. Meade, *Photonic crystals. Molding the flow of light* (Princeton University Press, 2008).

[5] P. A. Deymier, ed., *Acoustic metamaterials and phononic crystals* (Springer, 2013).

[6] O. N. Dorokhov, "On the coexistence of localized and extended electronic states in the metallic phase," Solid State Commun. **51**, 381 (1984).

[7] Y. Imry, "Active transmission channels and universal conductance fluctuations," Europhys. Lett. **1**, 249 (1986).

[8] P. A. Mello, P. Pereyra, and N. Kumar, "Macroscopic approach to multichannel disordered conductors," Ann. Phys. **181**, 290 (1988).

[9] Y. V. Nazarov, "Limits of universality in disordered conductors," Phys. Rev. Lett. **73**, 134 (1994).

[10] C. W. J. Beenakker, "Random-matrix theory of quantum transport," Rev. Mod. Phys. **69**, 731 (1997).

[11] W. Choi, A. P. Mosk, Q.-H. Park, and W. Choi, "Transmission eigenchannels in a disordered medium," Phys. Rev. B **83**, 134207 (2011).

[12] A. Goetschy and A. D. Stone, "Filtering random matrices: The effect of incomplete channel control in multiple scattering," Phys. Rev. Lett. **111**, 063901 (2013).

[13] B. Gérardin, J. Laurent, A. Derode, C. Prada, and A. Aubry, "Full transmission and reflection of waves propagating through a maze of disorder," Phys. Rev. Lett. **113**, 173901 (2014).

[14] R. Sarma, A. Yamilov, S. Petrenko, Y. Bromberg, and H. Cao, "Control of energy density inside a disordered medium by coupling to open or closed channels," Phys. Rev. Lett. **117**, 086803 (2016).

[15] I. M. Vellekoop and A. P. Mosk, "Focusing coherent light through opaque strongly scattering media," Opt. Lett. **32**, 2309 (2007).

[16] K. Vynck, R. Pierrat, R. Carminati, L. S. Froufe-Pérez, F. Scheffold, R. Sapienza, S. Vignolini, and J. J. Sáenz, "Light in correlated disordered media," arXiv:2106.13892 (2021).

[17] M. Davy, C. Ferise, É. Chéron, S. Félix, and V. Pagneux, "Experimental evidence of enhanced broadband transmission in disordered systems with mirror symmetry," Applied Physics Letters **119**, 141104 (2021), https://doi.org/10.1063/5.0062678.

[18] H. Zhang, H. Chu, H. Giddens, W. Wu, and Y. Hao, "Experimental demonstration of luneburg lens based on hyperuniform disordered media," Applied Physics Letters **114**, 053507 (2019), https://doi.org/10.1063/1.5055295.

[19] H. Zhang, Q. Cheng, H. Chu, O. Christogeorgos, W. Wu, and Y. Hao, "Hyperuniform disordered distribution metasurface for scattering reduction," Applied Physics Letters **118**, 101601 (2021), https://doi.org/10.1063/5.0041911.

[20] J. H. Weijs, R. Jeanneret, R. Dreyfus, and D. Bartolo, "Emergent hyperuniformity in periodically driven emulsions," Phys. Rev. Lett. **115**, 108301 (2015).

[21] A. Chremos and J. F. Douglas, "Hidden hyperuniformity in soft polymeric materials," Phys. Rev. Lett. **121**, 258002 (2018).

[22] S. Torquato and F. H. Stillinger, "Local density fluctuations, hyperuniformity, and order metrics," Phys. Rev. E **68**, 041113 (2003).

[23] R. D. Batten, F. H. Stillinger, and S. Torquato, "Classical disordered ground states: Super-ideal gases and stealth and equi-luminous materials," J. Appl. Phys. **104**, 033504 (2008).

[24] M. Florescu, S. Torquato, and P. J. Steinhardt, "Designer disordered materials with large, complete photonic band gaps," PNAS **106**, 20658 (2009).

[25] G. Zhang, F. H. Stillinger, and S. Torquato, "Ground states of stealthy hyperuniform potentials: I. entropically favored configurations," Phys. Rev. E **92**, 022119 (2015).

[26] G. Zhang, F. H. Stillinger, and S. Torquato, "Ground states of stealthy hyperuniform potentials. ii. stacked-slider phases," Phys. Rev. E **92**, 022120 (2015).

[27] O. Leseur, R. Pierrat, and R. Carminati, "High-density hyperuniform materials can be transparent," Optica **3**, 763 (2016).

[28]L. S. Froufe-Pérez, M. Engel, P. F. Damasceno, N. Muller, J. Haberko, S. C. Glotzer, and F. Scheffold, "Role of short-range order and hyperuniformity in the formation of band gaps in disordered photonic materials," Phys. Rev. Lett. **117**, 053902 (2016).

[29]L. S. Froufe-Pérez, M. Engel, J. J. Sáenz, and F. Scheffold, "Band gap formation and Anderson localization in disordered photonic materials with structural correlations," PNAS **114**, 9570 (2017).

[30]S. Torquato, "Hyperuniform states of matter," Phys. Rep. **745**, 1 (2018).

[31]F. Bigourdan, R. Pierrat, and R. Carminati, "Enhanced absorption of waves in stealth hyperuniform disordered media," Opt. Exp. **27**, 8666 (2019).

[32]G. J. Aubry, L. S. Froufe-Pérez, U. Kuhl, O. Legrand, F. Scheffold, and F. Mortessagne, "Experimental tuning of transport regimes in hyperuniform disordered photonic materials," Phys. Rev. Lett. **125**, 127402 (2020).

[33]A. Rohfritsch, J.-M. Conoir, T. Valier-Brasier, and R. Marchiano, "Impact of particle size and multiple scattering on the propagation of waves in stealthy-hyperuniform media," Phys. Rev. E **102**, 053001 (2020).

[34]A. Sheremet, R. Pierrat, and R. Carminati, "Absorption of scalar waves in correlated disordered media and its maximization using stealth hyperuniformity," Phys. Rev. A **101**, 053829 (2020).

[35]V. Romero-García, E. Chéron, S. Kuznetsova, J.-P. Groby, S. Félix, V. Pagneux, and L. M. García-Raffi, "Wave transport in 1d stealthy hyperuniform phononic materials made of non-resonant and resonant scatterers," APL Mater. **9**, 101101 (2021).

[36]V. Romero-García, N. Lamothe, G. Theocharis, O. Richoux, and L. M. García-Raffi, "Stealth acoustic materials," Phys. Rev. Appl. **11**, 054076 (2019).

[37]E. Chéron, J.-P. Groby, V. Pagneux, S. Félix, and V. Romero-García, "Experimental characterization of rigid scatterer hyperuniform distributions for audible acoustics," arXiv:2111.15548 (2021).

[38]W. Man, M. Florescu, E. P. Williamson, Y. He, S. R. Hashemizad, B. Y. C. Leung, D. R. Liner, S. Torquato, P. M. Chaikin, and P. J. Steinhardt, "Isotropic band gaps and freeform waveguides observed in hyperuniform disordered photonic solids," PNAS **110**, 15886 (2013).

[39]N. W. Ashcroft and N. D. Mermin, *Solid State Physics* (Saunders College Publishing, 1976).

[40]S. Kuznetsova, J.-P. Groby, L. M. García-Raffi, and V. Romero-García, "Stealth and equiluminous materials for scattering cancellation and wave diffusion," Waves Random Complex Media (published online, 2021).

[41]Y. Imry and R. Landauer, "Conductance viewed as transmission," Rev. Mod. Phys. **71**, S306 (1999).

[42]N. Verrier, L. Depraeter, D. Felbacq, and M. Gross, "Measuring enhanced optical correlations induced by transmission open channels in a slab geometry," Phys. Rev. B **93**, 161114 (2016).

[43]Note that the "Ohm" conductance varies with the frequency (see, in Figs. 3(a,e,i), the values of the conductance for $\chi \ll 1$), since the transport mean free path itself depends on the frequency.